Stability and dynamics of a plastic softening oscillator

Noël Challamel [a], Gilles Pijaudier-Cabot [b]

[a] *Laboratoire de Génie Civil et Génie Mécanique—LGCGM, INSA de Rennes, 20 avenue des Buttes de Coësmes, 35043 Rennes Cedex, France*

[b] *R&DO—GeM, Institut de recherches en Génie Civil et Mécanique, Ecole Centrale de Nantes, 1 rue de la Noë, 44321 Nantes Cedex 3, France*

This paper deals with the stability of a single-degree-of-freedom plastic softening oscillator. Understanding such an elementary model concerns, for instance, the seismic behaviour of concrete or steel structures. The associated dynamic system is a complex hysteretic system. Using appropriate internal variables, it can be written as a singular autonomous system. Liapounov stability of the solutions is then studied. A domain of perturbations associated with a stable solution is exhibited. This domain looks like a truncated cone in the three-dimensional phase space. It can be read as a critical displacement or energy that the oscillator can support during a seismic excitation. The difference with the ''equivalent'' linearized elastic system is highlighted. The unloading part of the response of the inelastic system has a stabilising effect.

Keywords: Stability of inelastic systems; Non-linear dynamics; Softening; Seismic design; Concrete structures; Steel structures; Large displacements

1. Introduction

The study of softening behaviour, which is characterised by a negative stiffness or a loss in strength after reaching a critical load-carrying capability, has benefited from extensive coverage in the research literature over the last two decades. This phenomenon is generally associated with the collapse of steel structures (Maier and Zavelani, 1970) or concrete structures (Bazant, 1976). It cannot be avoided when designing civil engineering structures to resist earthquake, especially when inelasticity occurs for large displacements or large strains. Up-to-now, many questions regarding how these structures behave during earthquakes remain unanswered. These questions are related to complex notions as stability, inelasticity and dynamic response which can be studied using Liapounov theory of stability. This paper comprises a tour through the issues of Liapounov

stability of inelastic softening systems. The developments herein are focused on the illustrative model of a single-degree-of-freedom oscillator.

Most geomaterials are characterised by softening for large deformations. Typical strain softening materials are rocks or concrete in tension and in compression at low confinement. For continuous media, this rheological specificity is associated with a "material instability" in the sense that uniqueness of the quasi-static evolution problem is no longer guaranteed (Hill, 1958). Softening induces a negative tangent stiffness matrix, and then boundary value problems (or initial value problems in dynamics) become ill-posed. Results depend strongly on the size of the localization zone (Bazant, 1976) and a localization limiter is often introduced in the rheology. Regularized models are most often non-local models (Pijaudier-Cabot and Bazant, 1987), gradient models (De Borst and Mühlhaus, 1992) or micropolar models (Vardoulakis and Sulem, 1995).

Stability and uniqueness criteria are thus often considered as the key problems in the modelling of these inelastic media (Bazant, 1988; Bazant and Cedolin, 2003). Nevertheless, the general criteria are not clearly related to stability in the sense of Liapounov: extensions of the famous second variation criterion generally used for non-linear elastic systems (Knops and Wilkes, 1973; Como and Grimaldi, 1995) have been investigated but the validity of such criteria including internal variables is still an open problem for inelastic systems (Nguyen, 2000; Petryk, 2002). Stability in the sense of Liapounov expresses the uniform continuity of the associated dynamic system with respect to initial conditions: it is quite natural that most difficulties encountered in stability analyses pertain to the complexity of the associated dynamical system.

Dynamics of inelastic systems (plastic or damage systems) is a complex issue, essentially because these systems are hysteretical (Capecchi, 1993). A treatment of free oscillations of such systems is available in standard text books such as Minorsky (1947). It is sometimes preferred to reduce the structural analysis to a finite-degree-of-freedom system, in order to avoid the difficulties involved in continuum approaches (Challamel, 2003a). Such a reduction cannot capture dynamic localization as exhibited by Bazant and Jirasek (1996) for instance. The choice of the present study is clearly not to cover all the complexities of continuous non-linear media, which can exhibit chaos even in elasticity (Holmes and Marsden, 1981; Davies and Moon, 1996). It is only to show, with a very simple model, the basic phenomena induced by softening inelasticity. In the same spirit, most studies are devoted to single-degree-of-freedom plastic oscillators in the literature. The work of Caughey (1960) is a pioneering analytical work, based on an equivalent asymptotic method to approximate the response of a plastic–kinematic hardening oscillator loaded by a harmonic function. Periodic motion has been found again with numerical simulations in the more general case of a mixed isotropic–kinematic hardening plastic oscillator (Savi and Pacheco, 1997). Limit cycles have been highlighted for the free undamped kinematic-hardening system (Pratap et al., 1994a,b). The same oscillator loaded by a periodic function shows very rich dynamical phenomena, and sometimes chaotic motion (Pratap and Holmes, 1995). The connection between elasto-plastic shakedown and limit cycle has been shown recently (Challamel, 2005).

The first part of this paper deals with the description of the single-degree-of-freedom oscillator. We start with this very simple example and show that in both cases of finite deformation and material non-linearity, softening is encountered. It appears that the softening plastic oscillator covers many situations, especially encountered for steel or concrete structures. It is a generic structural model that is also associated with a single-degree-of-freedom softening bar. In this spirit, both structural or material dynamic softening analyses can be presented in a unified way. The forced dynamics of such an oscillator has been numerically studied by Jennings and Husid (1968), Bernal (1987), Maier and Perego (1992) or MacRae (1994) using realistic earthquake loads. Williamson and Hjelmstad (2001) or Williamson (2003) considered plastic–damage coupled effects. Ballio (1968), Sun et al. (1973) or Yu and Zheng (1992) use portrait phases analysis in order to characterise the nature of dynamics phenomena. Ballio (1968) focuses on the response of the periodic forced system whereas Sun et al. (1973) or Yu and Zheng (1992) study the free vibrations of the system, considering different types of perturbations. Dynamics of the damage softening oscillator has been studied by Challamel and Pijaudier-Cabot (2004).

The second part deals with the stability of this simple inelastic oscillator loaded by a constant tensile force. This system is hysteretic because its local behaviour does not depend solely on the actual displacement but also on the history of the oscillator motion. The specificity of such a system is shown and a comparison with an "equivalent" linearized elastic system, introduced sometimes in simplified approaches of stability is proposed. Stability of equilibrium positions of the inelastic system (an infinite number of solutions in fact) is analysed

from the dynamic response of the perturbed motion: stability is then referred to the mathematical framework introduced by Liapounov at the beginning of the last century (see e.g. La Salle and Lefschetz, 1961 or Hagedorn, 1978).

2. Single DOF oscillator

2.1. Softening model—elastic case

The most elementary model associated with softening is the non-linear elastic model considered in Fig. 1. This simple single-degree-of-freedom system comprises a rigid column of length L, a concentrated mass m at the top (with no angular inertia) and a rotational elastic linear spring of stiffness k at the base. The column is loaded by a vertical force P and a horizontal force H. The rotation θ characterises the motion of the system.

The case where only a vertical force acts on the column is studied first. The equation of motion of this autonomous undamped system is

$$mL^2\ddot{\theta} + M(\theta) = 0 \quad \text{with } M(\theta) = k\theta - PL\sin\theta \tag{1}$$

The static equilibrium solutions are obtained from:

$$\theta = \eta\sin\theta \quad \text{with} \begin{vmatrix} P_{\text{cr}} = \frac{k}{L} \\ \eta = \frac{P}{P_{\text{cr}}} \end{vmatrix} \tag{2}$$

$\theta_0 = 0$ is a trivial equilibrium solution of such a system. The number of solutions of Eq. (2) depends on the structural parameter η. For $\eta < 1$, there is only one equilibrium solution θ_0. This solution is stable according to Lejeune–Dirichlet theorem. For $\eta \geqslant 1$, the equilibrium solution is not unique; the system admits two other solutions: $(\theta_1, -\theta_1)$ with $\theta_1 \in]0;\pi[$ when $\eta \leqslant 2\pi$. $\eta = 1$ is a bifurcation point (Nguyen, 2000). It is easy to show, using Liapounov theorem on the linearised motion, that the trivial position is no longer stable for $\eta > 1$. The moment function $M(\theta)$ has been plotted in Fig. 2 for different values of η. When the applied load exceeds the critical load P_{cr}, the moment–rotation curve exhibits softening at the origin (negative initial slope).

The form of this curve can be quite different in presence of lateral force H. The equilibrium curve is obtained from:

$$M(\theta) = k\theta - PL\sin\theta - HL\cos\theta = 0 \tag{3}$$

The proportional loading is studied:

$$P = \kappa H \quad \text{with } \kappa \geqslant 0 \tag{4}$$

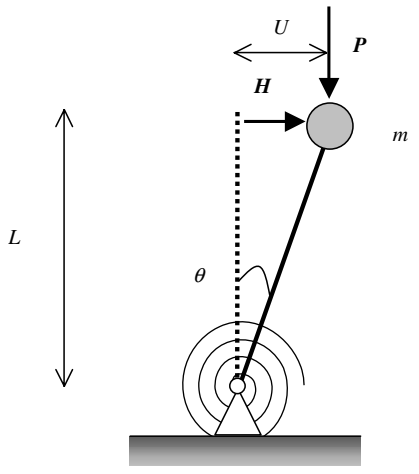

Fig. 1. Elastic buckling oscillator.

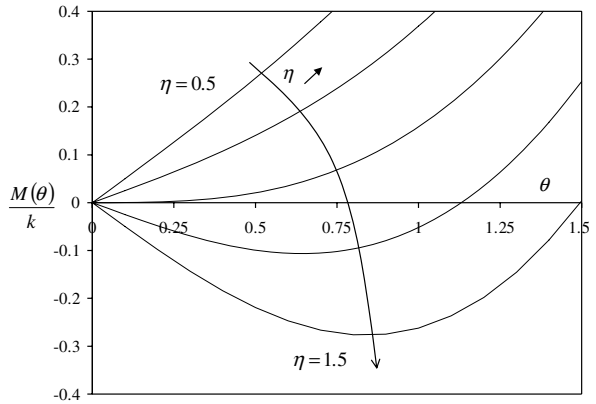

Fig. 2. Non-linear equivalent softening elastic relation—$H = 0$.

The relation between the lateral force and the rotation is given by:

$$\frac{H}{P_{\mathrm{cr}}} = \frac{\theta}{\kappa \sin\theta + \cos\theta} \tag{5}$$

Eq. (5) is plotted in Fig. 3. When κ is increasing, the slope of the load–rotation function is decreasing. The free dynamics of such a non-linear elastic system reduces to periodic motion, attractive trajectories or divergence motion. Nevertheless, in the presence of periodic loading, this simple system can exhibit very complex responses. Considering for instance the additional arbitrary harmonic solicitation (ω is the pulsation) which leads to the non-autonomous system:

$$mL^2\ddot{\theta} + k\theta - PL\sin\theta = HL\cos\omega t \tag{6}$$

It is often assumed for small rotations that

$$\sin\theta \approx \theta - \frac{\theta^3}{3!} \tag{7}$$

This new approximation yields the Duffing equation with negative linear stiffness when the load exceeds the elastic critical load:

$$mL^2\ddot{\theta} + k\left[(1-\eta)\theta + \eta\frac{\theta^3}{6}\right] = HL\cos\omega t \tag{8}$$

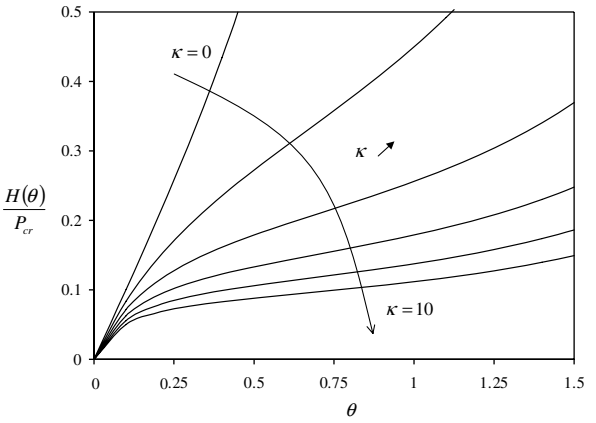

Fig. 3. Geometrical non-linear elastic relation—$P = \kappa H$.

This system can exhibit chaotic motion (Holmes, 1979; Guckenheimer and Holmes, 1987; Szemplinska-Stupnicka, 1988). Eqs. (6) or (8) are quite arbitrary since the excitation is chosen a priori. A much more physical horizontal harmonic force, for instance associated to a horizontal seismic load, would lead to another less studied system (Hjelmstad and Williamson, 1998):

$$mL^2\ddot{\theta} + k\theta - PL\sin\theta = HL\cos\theta\cos\omega t \tag{9}$$

The harmonic excitation could also affect the vertical loading:

$$mL^2\ddot{\theta} + k\theta - P\cos\omega t L\sin\theta = 0 \tag{10}$$

The linear approximation of Eq. (10) is the well-known Mathieu–Hill equation, associated to parametric resonance (Bolotin, 1963; Nayfeh and Mook, 1979):

$$mL^2\ddot{\theta} + k(1 - \eta\cos\omega t)\theta = 0 \tag{11}$$

Effects of the non-linear terms of Eq. (10) with respect to the linear Mathieu–Hill equation have been quantified by Mond et al. (1993). A very similar dynamic system was considered by McLaughlin (1981) and exhibits also chaotic phenomenon for a specific range of parameters. As a conclusion, even in case of linear elastic behaviour, complex dynamic phenomena may appear when such structural systems are loaded by seismic actions.

2.2. Softening model—elasto-plastic case

Inelastic analysis needs to be incorporated in order to model realistic structural collapse. Global softening, that is a structural response with a negative slope, may be induced by geometrical non-linearities (as noticed for steel frames during collapse) or by material softening (generally assumed for concrete cracking). The geometrical structural non-linearity is presented first. The material is assumed to be elastic–perfectly plastic. The analysis is conducted in large displacements for the column in Fig. 1. The spring has a perfect elasto-plastic behaviour with yield moment M_p. This academic case has been considered by Bernal (1987), MacRae (1994) or Aschheim and Montes (2003). Second-order analysis is performed only ($\theta \ll 1$). In the elastic phase, the equation of motion (1) including the lateral force (3) reduces to

$$m\ddot{U} + F(U) = H \quad \text{with } F(U) = \frac{k}{L^2}(1-\eta)U \tag{12}$$

where U is the lateral displacement of the top of the column. When the yield moment is reached, for monotonic loading ($\dot{U} \geqslant 0$), the motion is governed by

$$m\ddot{U} + F(U) = H \quad \text{with } F(U) = \frac{M_p}{L} - \eta\frac{k}{L^2}U \tag{13}$$

Unloading can also be described and the equivalent global restoring force F is in fact a linear plastic softening law (with kinematical softening). Such plastic softening law is represented in Fig. 4, only for positive force. Parameters of the plastic softening law can be calculated from the global characteristics of the oscillator:

$$\begin{vmatrix} F^+ = (1-\eta)\frac{M_p}{L} \\ U_Y = \frac{M_p}{P_{cr}} \end{vmatrix} \quad \text{and} \quad \begin{vmatrix} \frac{U_Y}{U_f} = \eta \\ K_0 = \frac{F^+}{U_Y} \end{vmatrix} \tag{14}$$

where F^+ is the limit force of the initial elastic domain and U_Y is the maximum displacement of the initial elastic domain. U_f is the displacement at failure obtained by setting $F(U_f) = 0$. It should be noted that the displacement at yield normalized by the failure displacement denoted here as η (and similar to what is often termed as "ductility") is equal to the ratio of buckling load P to the static buckling load P_{cr} defined in Eq. (2). K_0 is the elastic equivalent stiffness.

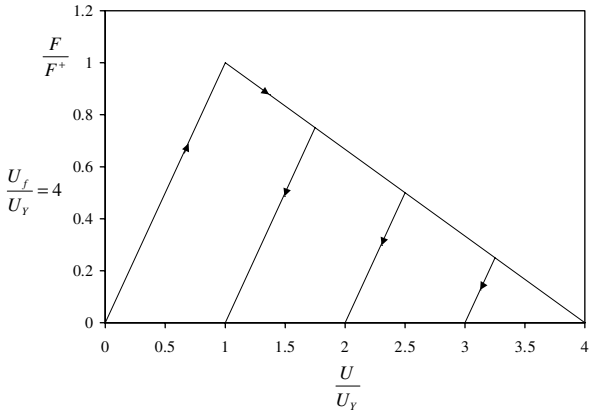

Fig. 4. Non-linear geometrical effects as a global elasto-plastic softening spring.

The equations of motion can finally be summarised as

$$m\ddot{U} + F(U, U_{\mathrm{p}}) = H \quad \text{with } F(U, U_{\mathrm{p}}) = K_0(U - U_{\mathrm{p}}) \tag{15}$$

where U_{p} is the plastic displacement. It is an internal variable of the elasto-plastic oscillator. The present result, dealing with the simple column free at the end, is also valid for other elementary single-degree-of-freedom systems. This is the case for instance of the frame considered in Fig. 5 (Ballio, 1970; Mazzolani and Piluso, 1996) where both elasto-plastic springs are identical.

Material non-linearity may yield strain softening too. This phenomenon (induced by microcracking) is observed for geomaterials such as rocks or concrete in tension and in compression for low confinement. Many strain softening models exist for three-dimensional media (see e.g. Jirasek and Bazant, 2002), plates (Belytschko and Fish, 1989) or beams (Bazant, 1976; Bazant et al., 1987). A plastic softening model is considered here.

The single-degree-of-freedom elasto-plastic beam model adopted by Pratap et al. (1994a,b) is useful to understand the consequences of material softening on stability (Fig. 6). The model consists in a mass m attached to two rigid links of length L. A softening elasto-plastic torsional spring (with linear softening) is attached at the mass point. θ is the rotation of the spring and U is the vertical displacement of the mass. This spring can physically be interpreted as a softening hinge. Assuming the displacements small, the equations of motion are:

$$\frac{mL^2}{4}\ddot{\theta} + M(\theta, \theta_{\mathrm{p}}) = \frac{HL}{2}; \quad U = \theta\frac{L}{2} \tag{16}$$

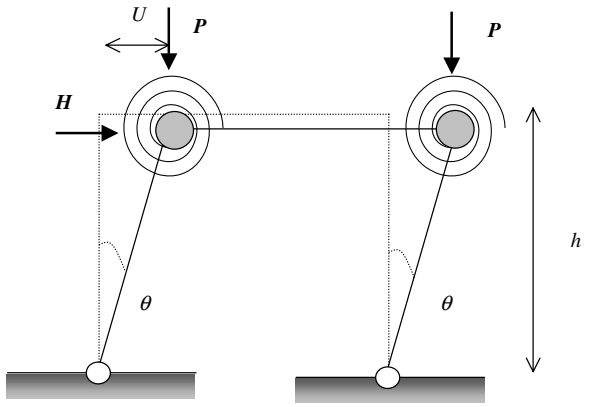

Fig. 5. Single-degree-of-freedom frame.

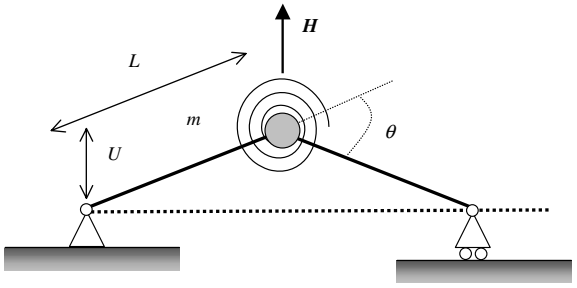

Fig. 6. Single-degree-of-freedom beam.

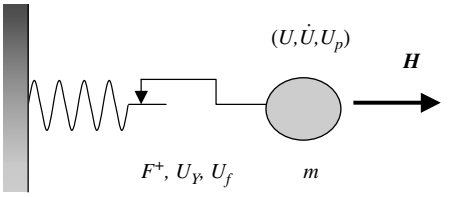

Fig. 7. Plastic softening oscillator.

The moment function M can be described according to a non-dimensional function similar to that in Fig. 4. θ_p is the plastic rotation of the plastic moment-rotation law. Eq. (16) can be reformulated to be the same as Eq. (15) without any difficulties. This system has been also studied by Ballio (1968) with a hardening rule coupled to geometrical non-linearity.

Steel beams can also be modelled, using "material" softening media for large rotations (Cocchetti and Maier, 2003). Local buckling prevails for large rotation values, depending on the cross-section classes (Mazzolani and Gioncu, 2002). It has been shown that the post-buckling behaviour can be described with a non-local softening media (Challamel, 2003b; Challamel and Hjiaj, 2005). Therefore, the generic softening plastic oscillator, as depicted in Fig. 7, covers many situations. It is also related to a single-degree-of-freedom softening bar and in this spirit, both structural or material dynamics softening analysis can be presented in a unified way.

3. Dynamics of the oscillator

3.1. Governing equations

Dynamics of the undamped inelastic oscillator in Fig. 7 is given by Eq. (15). The internal force F (constitutive law) depends on the actual position and on the plastic displacement. The incremental plastic law is illustrated in Fig. 8. The rheological model depends on three parameters: the elastic stiffness K_0, the maximum force F^+ and the failure displacement U_f. The limiting elastic displacement U_Y and the softening parameter η are also introduced from Eq. (14). In the simple case of the unsymmetric oscillator with infinite yield stress in compression, the internal variable reduces, for instance to the plastic displacement U_p. An equivalent quantity for this dynamic system is the history variable:

$$V(t) = \max_t U(t) \tag{17}$$

For the unsymmetric oscillator, the plastic displacement is

$$\left| \begin{array}{ll} U_p = V - U_Y \left\langle \frac{U_f - V}{U_f - U_Y} \right\rangle & \text{for } V \geqslant U_Y \\ U_p = 0 & \text{for } V < U_Y \end{array} \right. \tag{18}$$

where $\langle x \rangle = x$ if $x \geqslant 0$ and $\langle x \rangle = 0$ otherwise. Two states are distinguished in order to express the equations of motion explicitly. These two states correspond to a reversible state (or elastic state) denoted as $\widehat{E}$, and an

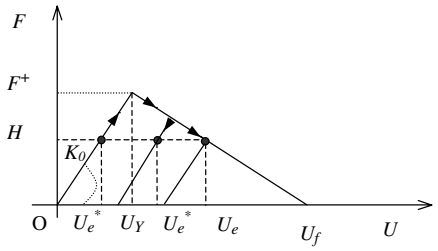

Fig. 8. Plastic law for the inelastic spring.

irreversible state (or plastic state) denoted as $\widehat{P}$. This differentiation is inspired from the works of Pratap et al. (1994a,b).

$$\left|\begin{array}{ll} \widehat{E} \text{ state:} & m\ddot{U} + K_0(U - U_{\mathrm{p}}(V)) = H \\ \widehat{P} \text{ state:} & m\ddot{U} + \left\langle \frac{F^+(U-U_{\mathrm{f}})}{U_{\mathrm{Y}}-U_{\mathrm{f}}} \right\rangle = H \end{array}\right. \tag{19}$$

These two states are distinguished by the following conditions:

$$\left|\begin{array}{ll} \widehat{E} \text{ state:} & (\dot{U} < 0) \text{ or } (\dot{U} \geqslant 0 \text{ and } U < V) \text{ or } (V < U_{\mathrm{Y}}) \\ \widehat{P} \text{ state:} & (\dot{U} \geqslant 0) \text{ and } (U = V) \text{ and } (V \geqslant U_{\mathrm{Y}}) \end{array}\right. \tag{20}$$

In particular, the dual variable $\dot{V}$ is ruled by equation:

$$\left|\begin{array}{ll} \widehat{E} \text{ state:} & \dot{V} = 0 \quad \text{if } V \geqslant U_{\mathrm{Y}} \\ \widehat{P} \text{ state:} & \dot{V} = \dot{U} \geqslant 0 \end{array}\right. \tag{21}$$

Such a representation is interesting because it shows the meaning of the internal variable and the type of dynamics involved by such a variable (note that a damage system would be very similar). The dynamic system can be now written as a simple autonomous system:

$$\dot{Q} = f(Q) \quad \text{with } Q = (U, \dot{U}, V) \tag{22}$$

The phase variables are $(U, \dot{U}, V)$. The function f can be deduced from Eqs. (19)–(21). In the case of linear softening considered in the paper, function f is a piecewise linear function. Such a choice allows the integrability of the system for each stage (also noticed by Aydinoglu and Fahjan, 2003). Nevertheless, as for most hysteretic systems, f is not differentiable.

It is clear that for a given fixed force H, an infinite number of static equilibrium solutions may exist for such a system. The set of equilibrium solutions U_{e}^* is continuous. In the case of non-linear elastic systems, this set would be discrete. Dynamics is studied in the neighbourhood of one of these solutions, a solution denoted by U_{e} (Fig. 8). It is the largest of all the solutions U_{e}^*. This solution is reputed to be unstable, or unstable in the sense of the linearized "equivalent" elastic solid (linear comparison solid, Hill, 1958). The following change of variable is chosen, in order to investigate the stability of the equilibrium position $(U = U_{\mathrm{e}}, V = V_{\mathrm{e}}, \dot{U} = \dot{U}_{\mathrm{e}} = 0)$:

$$\left|\begin{array}{l} u = \frac{U-U_{\mathrm{e}}}{U_{\mathrm{Y}}} \\ v = \frac{V-V_{\mathrm{e}}}{U_{\mathrm{Y}}}; \quad V_{\mathrm{e}} = U_{\mathrm{e}} \end{array}\right. \tag{23}$$

The new phase space is described by the new dimensionless variables:

$$q = (u, \dot{u}, v) \tag{24}$$

v is still associated to the history variable. The characteristic time of the system is defined as

$$t^* = \sqrt{\frac{m}{K_0}} \tag{25}$$

New temporal derivatives are written directly with respect to the dimensionless time parameter:

$$\tau = \frac{t}{t^*} \tag{26}$$

For elastic vibrations, the governing system of equations reads now:

$$\widehat{E} \text{ state: } \begin{vmatrix} \ddot{u} + u + \frac{U_{\mathrm{p,e}} - U_{\mathrm{p}}(v)}{U_{\mathrm{Y}}} = 0 \\ v = \max_{\tau} u(\tau); \; U_{\mathrm{p,e}} = U_{\mathrm{p}}(v = 0) \end{vmatrix} \tag{27}$$

From Eq. (18), the plastic displacement function is expressed by

$$\begin{vmatrix} U_{\mathrm{p}}(v) = U_{\mathrm{Y}} v + V_{\mathrm{e}} - U_{\mathrm{Y}} \left\langle \frac{U_{\mathrm{f}} - U_{\mathrm{Y}} v - V_{\mathrm{e}}}{U_{\mathrm{f}} - U_{\mathrm{Y}}} \right\rangle \quad \text{for } v \geqslant 1 - \frac{V_{\mathrm{e}}}{U_{\mathrm{Y}}} \\ U_{\mathrm{p}}(v) = 0 \quad \text{for } v < 1 - \frac{V_{\mathrm{e}}}{U_{\mathrm{Y}}} \end{vmatrix} \tag{28}$$

The plastic state is characterised by

$$\widehat{P} \text{ state: } \quad \ddot{u} + \left\langle -\frac{\eta}{1-\eta} u + \frac{H}{F^+} \right\rangle = \frac{H}{F^+} \tag{29}$$

and the two states can be distinguished by the conditions:

$$\begin{vmatrix} \widehat{E} \text{ state: } \quad (\dot{u} < 0) \text{ or } (\dot{u} \geqslant 0 \text{ and } u < v) \text{ or } (v < 1 - \frac{V_{\mathrm{e}}}{U_{\mathrm{Y}}}) \\ \widehat{P} \text{ state: } \quad (\dot{u} \geqslant 0) \text{ and } (u = v) \text{ and } \left(v \geqslant 1 - \frac{V_{\mathrm{e}}}{U_{\mathrm{Y}}}\right) \end{vmatrix} \tag{30}$$

These conditions are analogous to stick-slip conditions in frictional dynamic systems. Eq. (21) is rewritten as

$$\begin{vmatrix} \widehat{E} \text{ state: } \quad \dot{v} = 0 \quad \text{if } v \geqslant 1 - \frac{V_{\mathrm{e}}}{U_{\mathrm{Y}}} \\ \widehat{P} \text{ state: } \quad \dot{v} = \dot{u} \geqslant 0 \end{vmatrix} \tag{31}$$

3.2. Dynamics of the oscillator about $U = U_e$

The stability of the equilibrium position $q_{\mathrm{e}} = (u_{\mathrm{e}}, \dot{u}_{\mathrm{e}}, v_{\mathrm{e}}) = (0, 0, 0)$ is now studied from the perturbation $q_0 = (u_0, \dot{u}_0, v_0)$. Considering a perturbation constrained by $v_0 = 0$, it is easy to show that the motion necessarily diverges: the origin is unstable. This perturbation is an elastic perturbation, in the sense that the memory variable v has not been perturbed. A perturbation constrained by $v_0 > 0$ provides the same result. On the opposite side, considering $v_0 < 0$, the qualitative behaviour of the dynamics system strongly depends on the level of the perturbation. For sufficiently small perturbations inside a specific domain, equilibrium of the origin point remains stable. The meaning of a perturbation constrained by $v_0 < 0$ can be physically debated. It corresponds in fact to the stability of the origin, assuming that the material history authorised such a perturbed position. It necessarily means that the equilibrium position q_{e} was not reached in the past. This position is of course not always compatible with the loading history. The following perturbation is assumed:

$$\begin{vmatrix} u_0 = v_0 < 0, \\ \dot{u}_0 < 0, \end{vmatrix} \quad v_0 \geqslant 1 - \frac{U_{\mathrm{e}}}{U_{\mathrm{Y}}} \tag{32}$$

Other perturbations are deduced from this reference configuration. Perturbation (32) induces an elastic dynamic state:

$$\widehat{E} \text{ state: } \begin{vmatrix} \ddot{u} + u + \frac{U_{\mathrm{p,e}} - U_{\mathrm{p}}(v_0)}{U_{\mathrm{Y}}} = 0 \\ U_{\mathrm{p}}(v_0) < U_{\mathrm{p,e}} < U_{\mathrm{f}} \end{vmatrix} \tag{33}$$

The solution of the linear differential equation (33) has the classical form:

$$u(\tau) = R\cos(\tau - \varphi) + u^*; \quad v(\tau) = v_0 \qquad \text{where } u^* = \frac{U_{\mathrm{p}}(v_0) - U_{\mathrm{p,e}}}{U_{\mathrm{Y}}} \tag{34}$$

u^* is constant during the elastic phase. The constants R and φ are obtained from the initial conditions:

$$\left| \begin{array}{l} R^2 = \dot{u}_0^2 + (v_0 - u^*)^2 \\ \varphi = -a\cos\left(\frac{v_0 - u^*}{R}\right) \end{array} \right. \tag{35}$$

In the phase space, the trajectory is spherical and contained in the plane $v = v_0$. The time τ_1 necessary to initiate a plastic phase is computed from

$$\left| \begin{array}{l} u(\tau_1) = u_0 = v_0 < 0 \\ \dot{u}(\tau_1) = -\dot{u}_0 > 0 \end{array} \right. \tag{36}$$

During this plastic phase, the solution $u(\tau)$ is expressed on a exponential basis:

$$u(\tau) = C_1 \mathrm{e}^{-\sqrt{\frac{\eta}{1-\eta}}\tau} + C_2 \mathrm{e}^{\sqrt{\frac{\eta}{1-\eta}}\tau}; \quad v(\tau) = u(\tau) \tag{37}$$

Initial conditions give the constants C_1 and C_2:

$$\left| \begin{array}{l} C_1 = \frac{1}{2}\sqrt{\frac{1-\eta}{\eta}}\left(\dot{u}_0 + \sqrt{\frac{\eta}{1-\eta}}v_0\right)\mathrm{e}^{\sqrt{\frac{\eta}{1-\eta}}\tau_1} \\ C_2 = \frac{1}{2}\sqrt{\frac{1-\eta}{\eta}}\left(-\dot{u}_0 + \sqrt{\frac{\eta}{1-\eta}}v_0\right)\mathrm{e}^{-\sqrt{\frac{\eta}{1-\eta}}\tau_1} \end{array} \right. \tag{38}$$

Three types of dynamic responses can be distinguished from the sign of constant C_2. A critical velocity is then introduced:

$$\dot{u}_{\mathrm{c}} = \sqrt{\frac{\eta}{1-\eta}}|v_0| > 0 \tag{39}$$

The size of the perturbation governs the stability of the origin:

$$\left| \begin{array}{l} |\dot{u}_0| > \dot{u}_{\mathrm{c}} \;\Rightarrow\; \lim\limits_{\tau\to\infty} u(\tau) = \infty \\ |\dot{u}_0| = \dot{u}_{\mathrm{c}} \;\Rightarrow\; \lim\limits_{\tau\to\infty} u(\tau) = 0 \\ |\dot{u}_0| < \dot{u}_{\mathrm{c}} \;\Rightarrow\; \text{stationary periodic regime} \end{array} \right. \tag{40}$$

In the last case, another elastic phase is initiated and the motion is periodic. Purely elastic perturbations can also be studied. It is the case of the following perturbations:

$$\dot{u}_0^2 + (u_0 - u^*)^2 \leqslant (v_0 - u^*)^2 \tag{41}$$

Let us consider for instance:

$$\left| \begin{array}{l} 2u^* - v_0 \leqslant u_0 \leqslant v_0 < 0 \\ \dot{u}_0 = 0 \end{array} \right. \tag{42}$$

During the elastic phase, the equation of motion are directly written as

$$u(\tau) = (u_0 - u^*)\cos\tau + u^*; \quad v(\tau) = v_0 \tag{43}$$

and the dynamic system admits an other fixed point:

$$u(\tau) = u^*; \quad v(\tau) = v_0 \tag{44}$$

Dynamics of such an hysteretic system can be reduced to a periodic regime (after a certain time), attractive or divergent trajectories. These three cases are distinguished by the value of the initial speed $\dot{u}_0$ with respect to the critical speed $\dot{u}_{\mathrm{c}}$. The different types of dynamics are plotted in Fig. 9. For the simulations, parameters are chosen as

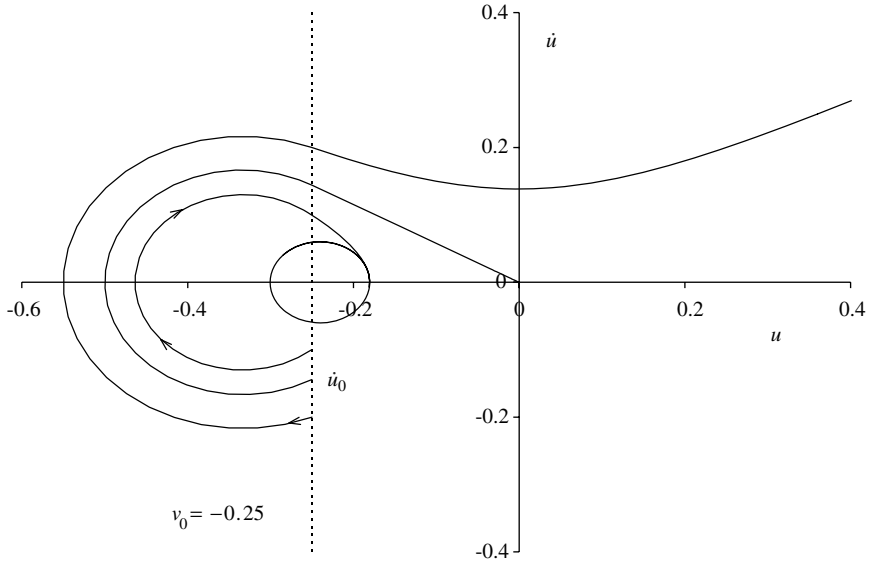

Fig. 9. Types of dynamics function of the perturbation.

$$\frac{H}{F^+} = 0.5; \quad \eta = 0.25 \Rightarrow \frac{U_e}{U_Y} = 2.5; \quad \frac{U_{p,e}}{U_Y} = 2 \tag{45}$$

with the following initial conditions:

$$\begin{vmatrix} u_0 = -0.25 \\ \dot{u}_0 = -0.1 \\ v_0 = -0.25 \end{vmatrix}; \quad \begin{vmatrix} u_0 = -0.25 \\ \dot{u}_0 = -0.144 = -\dot{u}_c \\ v_0 = -0.25 \end{vmatrix} \text{ and } \begin{vmatrix} u_0 = -0.25 \\ \dot{u}_0 = -0.2 \\ v_0 = -0.25 \end{vmatrix} \tag{46}$$

The three types of motion are plotted in Fig. 9. For sufficient large perturbations, the motion diverges. On the opposite, for sufficiently small perturbations, the motion is described by a circular trajectory after a plastic phase: the motion becomes periodic. The intermediate trajectory represented in Fig. 9 is an attractive trajectory. It asymptotically converges towards the origin. These curves are the projection of the true trajectory in the plane $(u, \dot{u})$. The true motion is a spatial motion in the three-dimensional phase space $(u, \dot{u}, v)$, as indicated in Fig. 10. The attractive trajectory is a special case. It is in fact the limit of the perturbation domain generating bounded evolutions. As we will see next, it is also the limit of the domain associated to stability of the origin (in the sense of Liapounov).

3.3. Stability analysis

It is usually easier to show instability than stability of an equilibrium in a given neighbourhood of this solution. In fact, it is not sufficient to observe the bounded aspect of the trajectory to conclude on stability. One has also to show the uniform continuity of the motion with respect to initial conditions, in a neighbourhood of the studied solution. It means practically that the perturbed motion evolves as the perturbation. This is mathematically expressed by the condition:

$$\exists A > 0 / \sup_{\tau} \|q(\tau)\| \leqslant A\|q_0\| \tag{47}$$

The choice of a metric is indifferent for the stability study of discrete systems. Let us consider for instance the following norm:

$$\|q\| = \max(|\, u \,|, |\, \dot{u} \,|, |\, v \,|) \tag{48}$$

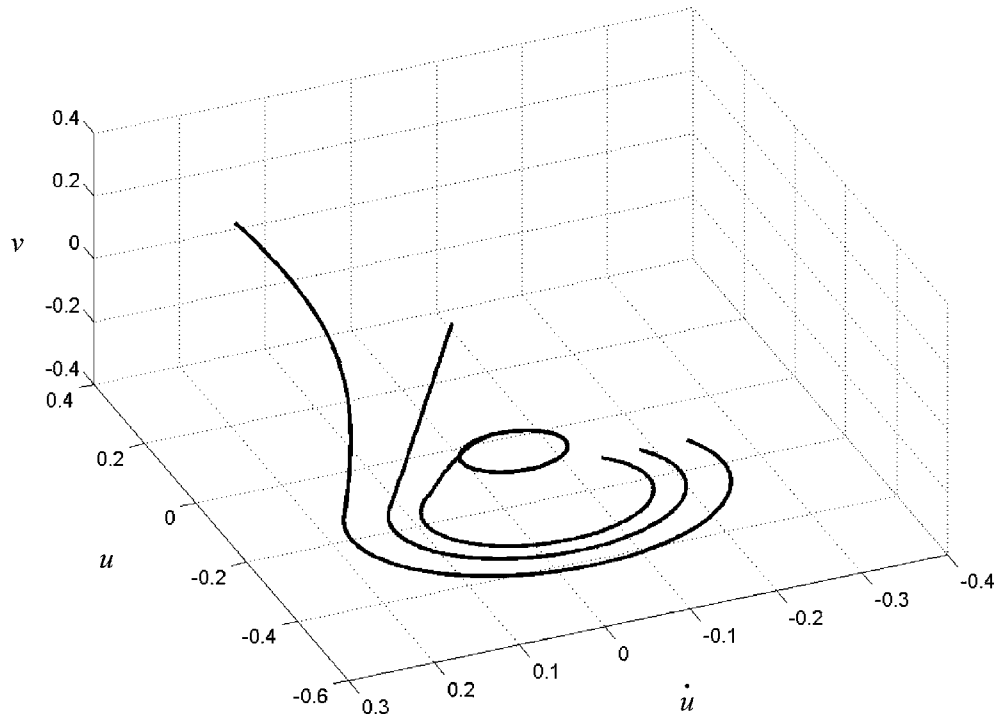

Fig. 10. Three-dimensional visualisation of the trajectory in the phase space.

Without loss of generality, the perturbation (42) is assumed for the proof of stability. The norm of this elastic perturbation is calculated from

$$\|q_0\| = \max(|\, u_0 \,|, |\, \dot{u}_0 \,|, |\, v_0 \,|) = |\, u_0 \,| = -u_0 \geqslant 0 \tag{49}$$

Equation of the perturbed motion is given in (43). This motion is bounded by

$$\begin{cases} \sup\limits_{\tau} |u(\tau)| = u_0 - 2u^*(v_0) \\ \sup\limits_{\tau} |\dot{u}(\tau)| = u_0 - u^*(v_0) \leqslant \sup\limits_{\tau} |u(\tau)| \end{cases} \tag{50}$$

The norm of the perturbed motion follows from

$$\sup_{\tau} \|q(\tau)\| = \sup_{\tau}[\max(|\, u(\tau) \,|, |\, \dot{u}(\tau) \,|, |\, v(\tau) \,|)] = \max[\sup_{\tau} |\, u(\tau) \,|, \sup_{\tau} |\, \dot{u}(\tau) \,|] \tag{51}$$

It can be noticed from Eq. (42) that

$$\frac{u^*}{u_0} \leqslant \frac{u^*}{v_0} \quad \text{with } u^*(v_0) \leqslant 0 \tag{52}$$

Finally, the ratio between the norm of the perturbed motion and the norm of the perturbation is given by

$$\frac{\sup\limits_{\tau} \|q(\tau)\|}{\|q_0\|} \leqslant g(v_0) \quad \text{with } g(v_0) = -1 + 2\frac{u^*(v_0)}{v_0} \tag{53}$$

With the numerical values of the parameters provided in Eq. (45), the function g is constant:

$$g(v_0) = \frac{5}{3} = A \tag{54}$$

It is sufficient to consider A as defined above to show the stability of the origin for the elastic perturbation. The proof is similar for the attractive trajectory or for the perturbation leading to a stationary periodic motion with a growth of the plastic displacement.

The boundary of the stability domain is defined by a circle (for v_0 fixed) truncated by the half-space:

$$u_0 \leqslant v_0 \tag{55}$$

The perturbation domain leading to stability of the origin is defined by:

$$\begin{vmatrix} \dot{u}_0^2 + (u_0 - u^*(v_0))^2 \leqslant \frac{\eta}{1-\eta} v_0^2 + (v_0 - u^*(v_0))^2 \\ u_0 \leqslant v_0 \end{vmatrix} \tag{56}$$

The stability domain is reduced to a point when $v_0 = 0$. This classical result of instability is recovered for this set of perturbations (a result widely accepted in the literature on strain softening). For $v_0 > 0$, there is no stability domain and instability is obtained whatever the perturbation. For $v_0 < 0$, a domain of perturbation leads to stability of the origin (Fig. 11). This stability domain looks like a truncated cone in a three-dimensional perturbations space (Fig. 12). The stability domain (perturbations domain leading to stability of the origin) of inelastic and equivalent elastic systems can be compared. The stability domain of the equivalent elastic system is reduced to a fixed point in the space $(u, \dot{u})$. In the case of an elastic material, the behaviour does not depend on the material history and the stability domain would be defined from:

$$\begin{vmatrix} u_0 = 0, \\ \dot{u}_0 = 0, \end{vmatrix} \quad v_0 \geqslant 0 \tag{57}$$

The difference between both domains (a volume for the inelastic system and a straight line for the elastic system) shows the "stabilising effect" of the inelastic system.

3.4. Dynamics of the oscillator about other equilibrium solutions

Stability of only one of the equilibrium solution has been studied (maximum of U_e^*). The previous results can be extended to the other equilibrium solutions denoted by U_e^* (Fig. 8). V_e^* is the history variable and it is not equal to U_e^*.

$$U_e^* \in \left[\frac{H}{K_0}; U_e\right] \quad \text{and} \quad U_e^* < V_e^* \tag{58}$$

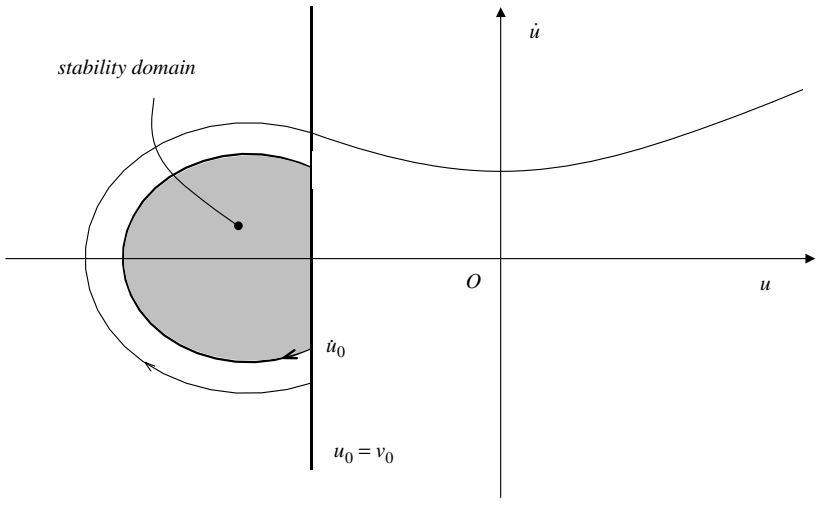

Fig. 11. Perturbations domain leading to stability of the origin.

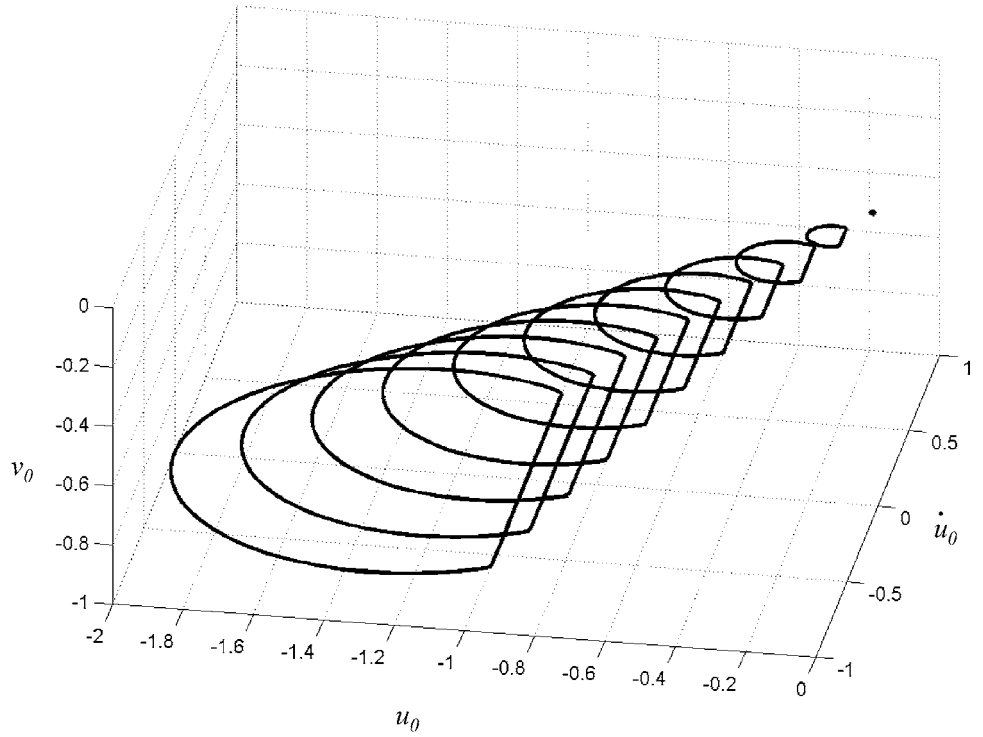

Fig. 12. Three-dimensional view of the stability domain.

The essential difference with the previous case is related to the existence of an elastic perturbation domain ($v_0 = 0$) associated to stability of the studied equilibrium solution. A new change of variable is implemented:

$$\left| \begin{array}{l} u = \frac{U - U_{\mathrm{e}}^*}{U_{\mathrm{Y}}} \\ v = \frac{V - V_{\mathrm{e}}^*}{U_{\mathrm{Y}}} \end{array} \right. \tag{59}$$

The relation between U_{e}^* and V_{e}^* is expressed in the form:

$$\frac{U_{\mathrm{e}}^*}{U_{\mathrm{Y}}} = \frac{H}{F^+} - \frac{1 - \frac{V_{\mathrm{e}}^*}{U_{\mathrm{Y}}}}{1 - \eta} \quad \text{with } V_{\mathrm{e}}^* \geqslant U_{\mathrm{Y}} \tag{60}$$

The dimensionless parameters are introduced as

$$\left| \begin{array}{l} u_{\mathrm{c}} = \frac{U_{\mathrm{c}} - U_{\mathrm{e}}^*}{U_{\mathrm{Y}}} > 0 \\ v^* = \frac{V_{\mathrm{e}}^* - U_{\mathrm{e}}^*}{U_{\mathrm{Y}}} > 0 \end{array} \right. \tag{61}$$

The two dynamics are then written with the new dimensionless variables:

$$\widehat{E} \text{ state:} \quad \left| \begin{array}{l} \ddot{u} + u + \frac{U_{\mathrm{p,e}}^* - U_{\mathrm{p}}(v)}{U_{\mathrm{Y}}} = 0 \\ v = \max_{\tau} u(\tau) - v^*; \quad U_{\mathrm{p,e}}^* = U_{\mathrm{p}}(v = 0) \end{array} \right. \tag{62}$$

This equation is similar to Eq. (27). The plastic displacement function is

$$\left| \begin{array}{l} U_{\mathrm{p}}(v) = U_{\mathrm{Y}} v + V_{\mathrm{e}}^* - U_{\mathrm{Y}} \left\langle \frac{U_{\mathrm{f}} - U_{\mathrm{Y}} v - V_{\mathrm{e}}^*}{U_{\mathrm{f}} - U_{\mathrm{Y}}} \right\rangle \quad \text{for } v \geqslant 1 - \frac{V_{\mathrm{e}}^*}{U_{\mathrm{Y}}} \\ U_{\mathrm{p}}(v) = 0 \quad \text{for } v < 1 - \frac{V_{\mathrm{e}}^*}{U_{\mathrm{Y}}} \end{array} \right. \tag{63}$$

and the expression of the plastic state changes to

$$\widehat{P} \text{ state:} \quad \ddot{u} + \left\langle -\frac{\eta}{1-\eta}(u-u_c) + \frac{H}{F^+} \right\rangle = \frac{H}{F^+} \tag{64}$$

The distinction between the two states (elastic and plastic) is now given by

$$\left| \begin{array}{l} \widehat{E} \text{ state:} \quad (\dot{u} < 0) \text{ or } (\dot{u} \geqslant 0 \text{ and } u < v + v^*) \text{ or } \left(v < 1 - \frac{V_e^*}{U_Y}\right) \\ \widehat{P} \text{ state:} \quad (\dot{u} \geqslant 0) \text{ and } (u = v + v^*) \text{ and } \left(v \geqslant 1 - \frac{V_e^*}{U_Y}\right) \end{array} \right. \tag{65}$$

Stability of the equilibrium position $q_e = (u_e, \dot{u}_e, v_e) = (0, 0, 0)$ is now studied. The following parameters have been chosen for the simulations of Fig. 13:

$$\frac{H}{F^+} = 0.5; \quad \eta = 0.25; \quad \frac{U_e^*}{U_Y} = 1.5 \Rightarrow \frac{U_e}{U_Y} = 2.5; \quad \frac{U_{p,e}^*}{U_Y} = 1; \quad u_c = 1; \quad v^* = 0.25 \tag{66}$$

with the initial conditions:

$$\left| \begin{array}{l} u_0 = 0.1 \\ \dot{u}_0 = 0 \\ v_0 = 0 \end{array} \right. ; \quad \left| \begin{array}{l} u_0 = 0.25 \\ \dot{u}_0 = 0 \\ v_0 = 0 \end{array} \right. ; \quad \left| \begin{array}{l} u_0 = 0.25 \\ \dot{u}_0 = -0.3 \\ v_0 = 0 \end{array} \right. ; \quad \left| \begin{array}{l} u_0 = 0.25 \\ \dot{u}_0 = -0.43 \\ v_0 = 0 \end{array} \right. \text{ and } \left| \begin{array}{l} u_0 = 0.25 \\ \dot{u}_0 = -0.55 \\ v_0 = 0 \end{array} \right. \tag{67}$$

These results can be generalised to perturbations in the form:

$$1 - \frac{V_e^*}{U_Y} \leqslant v_0 \leqslant u_c - v^* \tag{68}$$

It can be shown that the new stability domain is defined by the inequality:

$$\left| \begin{array}{l} \dot{u}_0^2 + (u_0 - u^*(v_0))^2 \leqslant \frac{\eta}{1-\eta}(u_c - v^* - v_0)^2 + (v_0 + v^* - u^*(v_0))^2 \\ u_0 \leqslant v_0 + v^* \end{array} \right.$$

with

$$u^*(v_0) = \frac{U_p(v_0) - U_{p,e}^*}{U_Y} \tag{69}$$

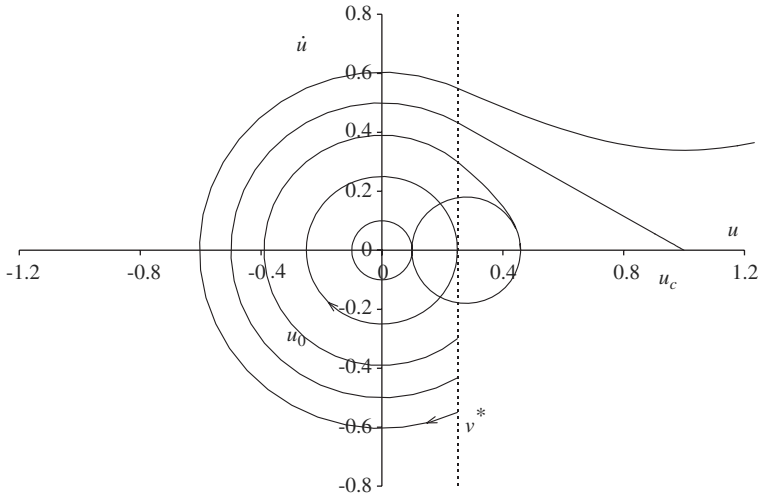

Fig. 13. Phase portraits—perturbations around U_e^*.

It is remarkable in this case that the origin is Liapounov stable considering a perturbation characterised by $v_0 > 0$. The size of the perturbations domain decreases as v_0 tends towards the characteristic value $u_c - v^*$. The perturbation domain (associated to the stability of the equilibrium solution) looks like a truncated cone. The origin point is included in this domain in the phase space (Fig. 14). The vertex of the cone corresponds to the other fixed point, whose coordinates are:

$$(u_0, \dot{u}_0, v_0) = (u_c, 0, u_c - v^*) \tag{70}$$

and the largest equilibrium solution U_e is recognised in this last equation.

3.5. Physical meaning

A simple instability criterion can then be deduced from Eq. (70), by remarking that

$$u_0 > u_c \iff U_0 > U_e \tag{71}$$

In this case, all equilibrium solutions are unstable in the sense of Liapounov (leading to divergence evolutions and then to collapse):

$$V_0 \geqslant U_0 > U_e \Rightarrow \text{Collapse} \tag{72}$$

Moreover, it can also be shown that

$$\exists t / U(t) > U_e \Rightarrow \text{Collapse} \tag{73}$$

The limit displacement U_e can be used as an indicator of the safety of the structure during the loading history. A particular case is the investigation of the stability of the smallest static equilibrium solution, denoted by U_S, e.g. for the service state of the structure (see Fig. 15).

$$U_S = \min U_e^* \tag{74}$$

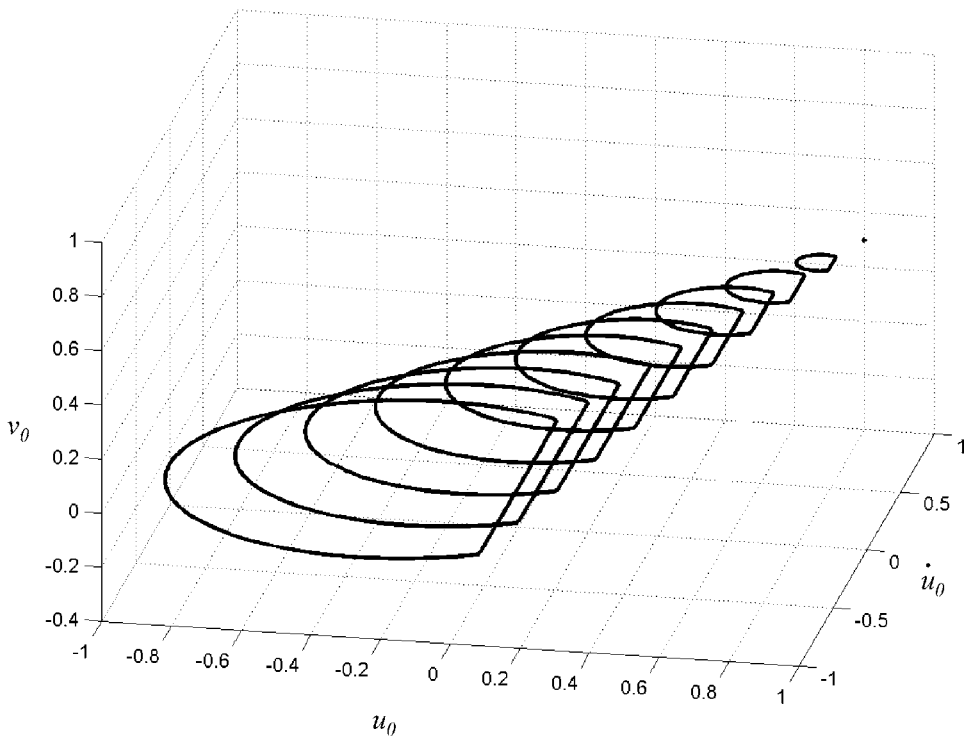

Fig. 14. Three-dimensional view of the stability domain—general case.

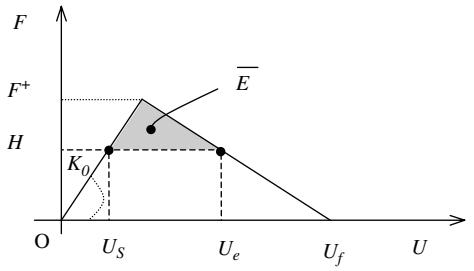

Fig. 15. Stability of the service state solution.

An elastic perturbation is considered and the equilibrium parameters are reduced to:

$$v_0 = 0; \quad V_e^* = U_Y; \quad \frac{U_e^*}{U_Y} = \frac{H}{F^+} \tag{75}$$

The stability domain, given by Eq. (69) is then simplified:

$$\dot{u}_0^2 + u_0^2 \leqslant \frac{1}{\eta}\left(1 - \frac{H}{F^+}\right)^2 \tag{76}$$

Eq. (76) can be converted using original displacement or time variables $(U_0, \dot{U}_0, t)$:

$$\frac{1}{2}m\dot{U}_0^2 + \frac{1}{2}K_0\left(U_0 - \frac{H}{K_0}\right)^2 \leqslant \frac{1}{\eta}\left(1 - \frac{H}{F^+}\right)^2 * \frac{1}{2}K_0 U_Y^2 \tag{77}$$

One recognizes clearly in Eq. (77) an energy in equation:

$$E_0 \leqslant \overline{E} \quad \text{with } \overline{E} = \frac{1}{\eta}\left(1 - \frac{H}{F^+}\right)^2 * \frac{1}{2}K_0 U_Y^2 \tag{78}$$

It means that the total energy E_0 induced by the seismic perturbation (summation of the potential and the kinetic energy) cannot exceed a threshold $\overline{E}$. In the opposite case, instability of the service state equilibrium solution prevails, and leads to collapse. The meaning of this critical energy is more readable, by considering graphical arguments of Fig. 15. In Fig. 15, the critical energy $\overline{E}$ is exactly equal to the dark area. The more ductile the plastic behaviour (low value of η), the highest the admissible seismic perturbation energy (perturbation domain associated to the stability of the equilibrium service state).

4. Conclusions

This paper deals with the stability of a single-degree-of-freedom plastic softening oscillator. It is shown in the first part that this generic structural model covers both material and geometrical softening. Understanding such an elementary model concerns for instance the seismic behaviour of concrete or steel structures.

The associated dynamic system is a complex hysteretic system. Using appropriate internal variables (plastic displacement or an equivalent memory variable), the dynamic system can be written as a singular autonomous system. Liapounov stability of the equilibrium solutions is then studied.

The inelastic system is compared to the "equivalent" linearized comparison solid. For every equilibrium solution of the inelastic system, a perturbation domain associated to stability exists. This domain looks like a truncated cone in the three-dimensional phases space. The present stability study confirms an intuitive idea: inelasticity has a stabilising effect. For seismic design applications, the stability domain (Eq. (69)) can be interpreted as a critical displacement or energy level (induced by seismic loads for instance) that the oscillator can support while remaining stable. For higher levels, a divergent evolution is noticed, leading to structural collapse. Such levels could also be converted into energy based quantities.

This study deals with a simple generic structural model, which may be helpful to understand many phenomena encountered in structural dynamics. Nevertheless, such an elementary model should be enriched in order

to describe more realistic structural frames. For instance, Bazant and Jirasek (1996) show the difficulty related to the reduction to a single-degree-of-freedom oscillator in the dynamics of softening media. Dynamic localization can be predominant and the previous simple model cannot capture such phenomenon. In case of softening beams (concrete or steel structural members), softening hinges have to be defined in connection with non-local plasticity formulation (Challamel, 2003a,b; Cocchetti and Maier, 2003). Stability of these non-local continuous media might be considered as an extension of this work.

References

Aschheim, M., Montes, E.H., 2003. The representation of *p*-delta effects using yield point spectra. Eng. Struct. 25, 1387–1396.

Aydinoglu, M.N., Fahjan, Y.M., 2003. A unified formulation of the piecewise exact method for inelastic seismic demand analysis including *P*-delta effect. Earthquake Eng. Struct. Dyn. 32, 871–890.

Ballio, G., 1968. Elastic–plastic dynamic behavior of a beam-column model. Meccanica 3, 177–186.

Ballio, G., 1970. On the dynamic behavior of an elastoplastic oscillator (experimental investigations and theoretical developments). Meccanica 5, 85–97.

Bazant, Z.P., 1976. Instability, ductility and size effect in strain-softening concrete. J. Eng. Mech. 102, 331–344.

Bazant, Z.P., 1988. Stable states and paths of structures with plasticity or damage. J. Eng. Mech. 114 (12), 2013–2034.

Bazant, Z.P., Cedolin, L., 2003. Stability of Structures—Elastic, Inelastic, Fracture and Damage Theories. Dover Publications, Inc., New York.

Bazant, Z.P., Jirasek, M., 1996. Softening-induced dynamic localization instability: seismic damage in frames. J. Eng. Mech. 122 (12), 1149–1158.

Bazant, Z.P., Pan, J., Pijaudier-Cabot, G., 1987. Softening in reinforced concrete beams and frames. J. Struct. Eng. 113, 2333–2347.

Belytschko, T., Fish, J., 1989. Embedded hinge lines for plate elements. Comput. Meth. Appl. Mech. Eng. 76, 67–86.

Bernal, D., 1987. Amplification factors for inelastic dynamic *p*-delta effects in earthquake analysis. Earthquake Eng. Struct. Dyn. 15, 635–651.

Bolotin, V.V., 1963. Nonconservative Problems of the Theory of Elastic Stability. Pergamon Press, New York.

Capecchi, D., 1993. Asymptotic motions and stability of the elastoplastic oscillator studied via maps. Int. J. Solids Struct. 30 (23), 3303–3314.

Caughey, T.K., 1960. Sinusoidal excitation of a system with bilinear hysteresis. J. Appl. Mech. 27 (4), 649–652.

Challamel, N., 2003a. Contribution of Liapounov stability theory to geomechanics. In: 16th Eng. Mech. Conf., Seattle.

Challamel, N., 2003b. Une approche de plasticité au gradient en construction métallique. C. R. Acad. Sci. 331 (9), 647–654.

Challamel, N., 2005. Dynamic analysis of elastoplastic shakedown of structures. Int. J. Struct. Stability Dyn. 5 (2), 259–278.

Challamel, N., Hjiaj, M., 2005. Non-local behaviour of plastic softening beams. Acta Mech. 178, 125–146.

Challamel, N., Pijaudier-Cabot, G., 2004. Stabilité et dynamique d'un oscillateur endommageable. Revue Française de Génie Civil 8 (4), 483–505.

Cocchetti, G., Maier, G., 2003. Elastic–plastic and limit-state analyses of frames with softening plastic-hinge models by mathematical programming. Int. J. Solids Struct. 40, 7219–7244.

Como, M., Grimaldi, A., 1995. Theory of Stability of Continuous Elastic Structures. CRC Press, 138 p.

Davies, M.A., Moon, F.C., 1996. Transition from soliton to chaotic motion following sudden excitation of a nonlinear structure. J. Appl. Mech. 63, 445–449.

De Borst, R., Mühlhaus, H.B., 1992. Gradient-dependent plasticity: formulation and algorithmic aspects. Int. J. Numer. Meth. Eng. 35, 521–539.

Guckenheimer, J.A., Holmes, P.J., 1987. Nonlinear Oscillations, Dynamical Systems and Bifurcations of Vector Fields. Springer, Berlin.

Hagedorn, P., 1978. Non-linear Oscillations. Oxford Science Publications, p. 283.

Hill, R., 1958. A general theory of uniqueness and stability in elastic–plastic solids. J. Mech. Phys. Solids 6, 236–249.

Hjelmstad, K.D., Williamson, E.B., 1998. Dynamic stability of structural systems subjected to base excitation. Eng. Struct. 20 (4–6), 425–432.

Holmes, P.J., 1979. A nonlinear oscillator with a strange attractor. Phil. Trans. R. Soc. Lond., Ser. A 292, 419–448.

Holmes, P.J., Marsden, J., 1981. A partial differential equation with infinitely many periodic orbits: chaotic oscillations of a forced beam. Arch. Rat. Mech. Anal. 76, 135–166.

Jennings, P.C., Husid, R., 1968. Collapse of yielding structures under earthquakes. J. Eng. Mech. Div., ASCE 94, 1045–1065.

Jirasek, M., Bazant, Z.P., 2002. Inelastic Analysis of Structures. Wiley, 758 p.

Knops, R.J., Wilkes, E.W., 1973. Theory of elastic stability. Handbuch der Physik Band Via/3. Springer-Verlag, New York, pp. 125–289.

La Salle, J., Lefschetz, S., 1961. Stability by Liapunov's Direct Method with Applications. Academic Press, New York, 134 p.

MacRae, G.A., 1994. P–Δ effects on single-degree-of-freedom structures in earthquakes. Earthquake Spectra 10 (3), 539–568.

Maier, G., Perego, U., 1992. Effects of softening in elastic–plastic structural dynamics. Int. J. Numer. Meth. Eng. 34, 319–347.

Maier, G., Zavelani, A., 1970. Sul comportamento di aste metaliche compresse eccentricamente. Indagine sperimentale e considerazioni teoriche. Costruzioni Metalliche 22 (4), 282–297.

Mazzolani, F.M., Gioncu, V., 2002. Ductility of Seismic-resistant Steel Structures. Spon Press, 720 p.

Mazzolani, F.M., Piluso, V., 1996. Theory and Design of Seismic Resistant Steel Frames. Chapman & Hall, 497 p.

McLaughlin, J.B., 1981. Period-doubling bifurcations and chaotic motion for a parametrically forced pendulum. J. Statist. Phys. 24 (2), 375–388.
Minorsky, N., 1947. Non-linear Mechanics. Edward Brothers, Michigan.
Mond, M., Cederbaum, G., Khan, P., Zarmi, Y., 1993. Stability analysis of the non-linear Mathieu equation. J. Sound Vibrat. 167 (1), 77–89.
Nayfeh, A.H., Mook, D.T., 1979. Non linear Oscillations. Pure & Applied Mathematics, A. Wiley, Interscience Series of Texts.
Nguyen, Q.S., 2000. Stabilité et mécanique non linéaire. Hermes, 461 p.
Petryk, H., 2002. Second-order work and dissipation on indirect paths. C. R. Mécanique 330, 121–126.
Pijaudier-Cabot, G., Bazant, Z.P., 1987. Non local damage theory. J. Eng. Mech., ASCE 113 (10), 1512–1533.
Pratap, R., Holmes, P.J., 1995. Chaos in a mapping describing elastoplastic oscillations. Nonlinear Dyn. 8, 111–139.
Pratap, R., Mukherjee, S., Moon, F.C., 1994a. Dynamic behavior of a bilinear hysteretic elasto-plastic oscillator, Part I: free oscillations. J. Sound Vibrat. 172 (3), 321–337.
Pratap, R., Mukherjee, S., Moon, F.C., 1994b. Dynamic behavior of a bilinear hysteretic elasto-plastic oscillator, Part II: oscillations under periodic impulse forcing. J. Sound Vibrat. 172 (3), 339–358.
Savi, M.A., Pacheco, P.M.C.L., 1997. Non-linear dynamics of an elasto-plastic oscillator with kinematic and isotropic hardening. J. Sound Vibrat. 207 (2), 207–226.
Sun, C.K., Berg, G.V., Hanson, R.D., 1973. Gravity effect on single-degree inelastic system. J. Eng. Mech. Div. 99, 183–200.
Szemplinska-Stupnicka, W., 1988. Bifurcations of harmonic solution leading to chaotic motion in the softening type Duffing's oscillator. Int. J. Non-Linear Mech. 23 (4), 257–277.
Vardoulakis, I., Sulem, J., 1995. Bifurcation Analysis in Geomechanics. Chapman and Hall, 462 p.
Williamson, E.B., 2003. Evaluation of damage and P-Δ effects for systems under earthquake excitation. J. Struct. Eng. 129 (8), 1036–1046.
Williamson, E.B., Hjelmstad, K.D., 2001. Nonlinear dynamics of a harmonically-excited inelastic inverted pendulum. J. Eng. Mech. 127 (1), 52–57.
Yu, Y., Zheng, J., 1992. Dynamic elastic–plastic buckling behavior illustrated by simple model. J. Eng. Mech. 118 (10), 2005–2016.